ENGINEERING MECHANICS 2004
NATIONAL CONFERENCE
with international participation
Svratka, Czech Republic, 10 - 13 May 2004

FLOW CONTROL USING SYNTHETIC JET ACTUATORS

V. Uruba*

Summary

A synthetic jet can be produced over broad range of time and length-scales. Theirs unique attributes make them attractive fluidic actuators for various flow-control tasks. Generation, evolution and interaction of synthetic jets are reviewed in the presented paper. Application of this actuator type ranging from separation and turbulence control, control to thrust vectoring and mixing augmentation to skin friction control is shown.

1. Introduction

Recently, many researchers (namely in the US) are interested in a synthetic jet research. The reason is potential possibility of using this type of actuators in flow control. Although, these actuators have not been used in practice yet, the MEMS technology development in recent years makes this principle very promising for using in various fluid dynamics control applications namely in aero-engineering.

Some authors refer to this phenomenon as a zero-net-mass-flux jet, unsteady bleeding, suction and blowing, oscillatory blowing, acoustic streaming etc. However, comparing with acoustic streaming there is a considerable difference. Acoustic streaming represents itself the generation of a mean motion by sound. These flows are very similar to synthetic jet flow in that they are zero net mass. However, a synthetic jet is not necessarily an acoustic streaming effect, since it does not rely on any acoustic effect, and it has a mean flow on the same order as the oscillatory orifice flow. Acoustic streaming cannot occur unless the fluid compresses, but a synthetic jet can be generated in a completely incompressible fluid.

An isolated synthetic jet is produced by the interactions of a train of vortices that are typically formed by alternating ejection and suction of fluid across an orifice in a wall such that the net mass flux is zero. Resulting jet is formed entirely from the working fluid of the flow system in which it is deployed and thus can transfer linear momentum to the flow system without net mass injection across the flow boundary.

Synthetic jets can be produced over a broad range of length and time-scales, they are attractive fluidic actuators for a broad range of flow control applications. A synthetic jet could be of circular or planar nominally 2D cross-section depending on the generators orifice shape. Planar synthetic jet using a slot orifice is more convenient for a 2D boundary layer control purposes, however the physics of both 2D and rotary symmetrical synthetic jets is analogous. Most of results presented in this review are related to a 2D synthetic jet.

* Ing.Václav Uruba, CSc, Institute of Thermomechanics, AS CR, E-mail: uruba@it.cas.cz

2. Synthetic Jet Physics

A generator consisting of a cavity with periodically moving boundary and orifice typically generates a synthetic jet – see schematics in Figure 1. A piston here represents moving boundary. Two generating phases are shown: a) blowing phase generating a vortex and b) suction phase producing pressure drop in the orifice region.

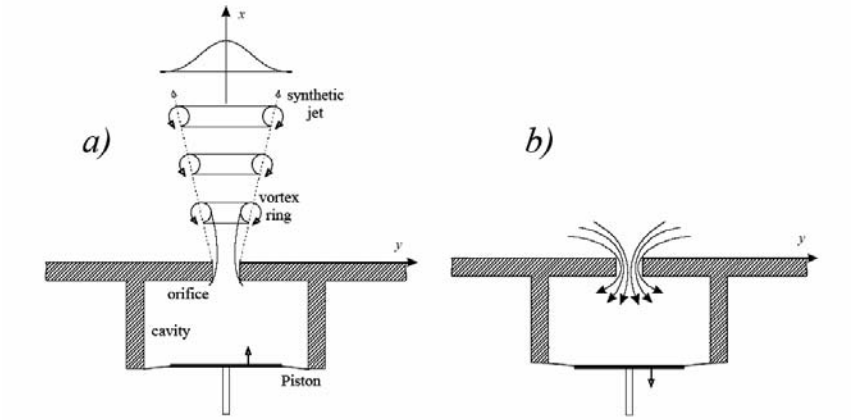

Fig.1 – Schema of synthetic jet generation
a) blowing, and *b)* suction phases

A synthetic jet flow field is generated by the advection and interactions of trains of discrete vortical structures (see e.g. [31]). The hydrodynamic impulse, which is necessary to form each of these vortices, originates at the flow boundary by the momentary discharge of slugs of fluid through an orifice. If the output flow velocity exceeds certain limit during the cycle, the flow separates at the edge of the orifice, and a vortex sheet is formed and rolls into an isolated vortex that is subsequently advected away under its own self-induced velocity. Depending on the flow regularity and the repetition rate, the dynamics and interactions of the vortical structures within a pulsed jet can lead to spatial evolution that is remarkably different from the evolution of a continuous (conventional) jet having the same orifice and time-averaged flux of streamwise momentum.

A crucial point of a synthetic jet generation process is formation of vortices. This mechanism has been studied thoroughly in past both experimentally and theoretically. In Figure 2 a series of subsequent stages of vortex ring formation is shown as a result of inviscid calculation [30]. Vortex ring could be produced by impulsively ejecting a slug of fluid through a circular tube orifice opening into a quiescent fluid, which is provoked e.g. by a moving piston. A detailed study of formation process shows that when a piston ejects fluid through the tube, Vorticity is generated on the inner wall of the tube due to the no-slip boundary condition. As this layer of Vorticity leaves the tube, it forms a cylindrical vortex sheet, which immediately rolls-up into a spiral. During this process the diameter of the surrounding fluid. Then the vortex reaches

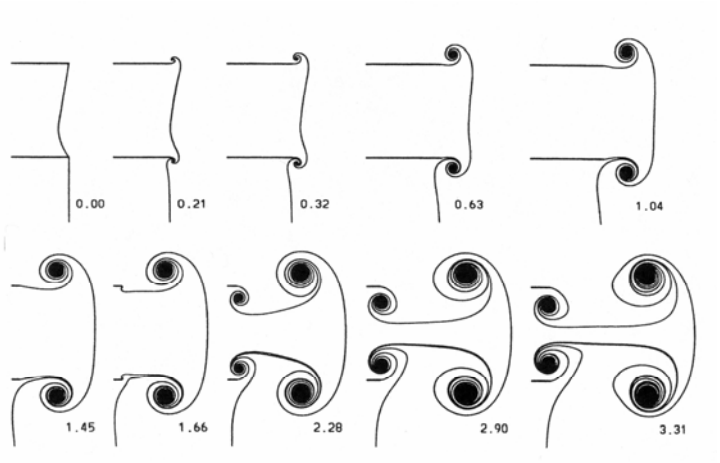

Fig.2 – Behaviour of cylindrical vortex sheet

certain size; it starts moving away from the nozzle (in the figure rightward). As soon as the piston stops, the secondary vortex is formed inside the orifice having opposite circulation. In the meantime, the main travelling vortex settles down the appropriate shape of oblate ellipsoid.

Synthetic jet flows are similar to pulsed jets in that they are also produced by the advection and interactions of trains of discrete vortical structures. However, a unique feature of synthetic jets is that they are formed entirely from the working fluid of the flow system in which they are deployed and thus they can transfer linear momentum to the flow system without net mass injection across the flow boundary. The fluid that is necessary to synthesize the jet is typically supplied by intermittent suction through the same flow orifice between consecutive ejections. Because the characteristic dimensions of the ensuing jet scale with the orifice, it is possible, in principle, to synthesize jets over a broad range of length scales.

An acoustic field can impose the oscillating, time-reversed pressure drop across an orifice that is necessary to form a synthetic jet, provided that the amplitude of the pressure oscillations is large enough to induce the time-periodic rollup and subsequent advection of discrete vortices. The impulse that is imparted to each vortex has to be large enough to overcome the influence of both the orifice image, and the forces associated with the reversed suction flow. Streaming motions without mass addition can also be effected by the transmission of sound through the flow field (often referred to as acoustic streaming) or by oscillating the boundary of a quiescent medium. Although these streaming flows are produced without net mass flux, they are not typically accompanied by the formation of discrete vortices that are inherent in the formation of synthetic jets by fluid injection through an orifice. As noted in [19], the streaming motions induced by acoustic waves result from the dissipation of acoustic energy or the attenuation of the transmitted sound. Such attenuation can occur either within the body of the fluid away from solid surfaces at very high frequencies, or owing to viscous effects near a solid boundary. Streaming motions associated with moving (oscillating) solid boundaries have been the subject of a number of investigations.

In recent years, plane and round synthetic jets that are formed by time-periodic alternate ejection and suction of the working fluid through an orifice in the flow boundary have been investigated both experimentally (e.g. [34], [15], [33], [36]) and numerically (e.g. [25], [28], [29]). The studies have shown that near the jet exit plane, the synthetic jet flow is dominated by the time-periodic formation, advection, and interactions of discrete vortical structures (e.g., vortex pairs or vortex rings), which finally become turbulent, slow down, and lose their coherence. As a result of the suction flow, the time-averaged static pressure near the exit plane of a synthetic jet is typically lower than the ambient pressure. Both the streamwise and cross-stream velocity components reverse their direction during the actuation cycle. The time-periodic reversal in flow direction along the jet centreline (between the blowing and

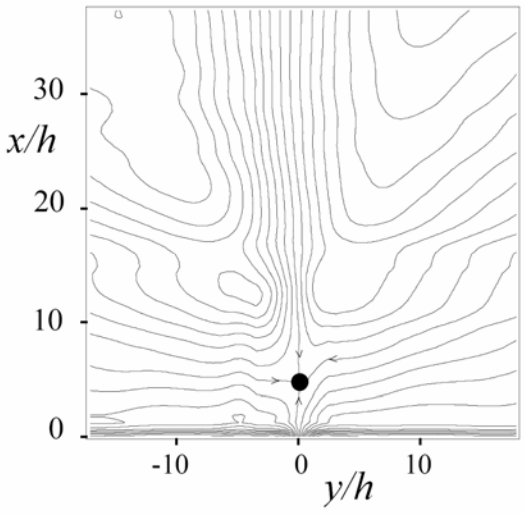

Fig.3 – Phase-averaged streamline map at $t/T = 0.75$

suction strokes) leads to the formation of a stagnation point on the centreline downstream of the orifice and confines the suction flow to a narrow domain near the exit plane. The situation is schematically depicted in Figure 3. These features as well as the celerity and characteristic length scale of the discrete vortices that form the jet can be varied over a broad range by the amplitude and period of the diaphragm motion.

The unique attributes of synthetic jets coupled with the development of actuators that can be integrated into the flow surface without the need for complex piping and fluidic packaging make them attractive fluidic actuators for control of both external and internal flows. As noted above, apparent surface modification is typically implemented by operating the jet actuator on timescales that are below the characteristic timescale of the base flow. However, the unsteady effects of the actuation can also be coupled to inherent instabilities of the base flow to affect significant global modifications on scales that are one to two orders of magnitude larger than the characteristic length scales of the jets themselves.

3. Scales and dimensionless parameters

In a synthetic jet generation process the important physical parameters are the relative importance of viscous effects, and the relative importance of unsteady effects.

Viscous effects are defined by Reynolds number, which is based on reference velocity $U_{\max}$, orifice characteristic dimension h (diameter or slot width) and fluid viscosity ν. The reference velocity could be e.g. maximum velocity of fluid in the orifice during the actuating period. Then the Reynolds number could be:

$$Re_{\max} = \frac{U_{\max}\, h}{\nu}. \qquad \{1\}$$

If this Reynolds number falls below a critical value, which could be from 10 to 50 according to actual configuration, the jet during the blowing period will not separate from the orifice edge and the flow will become reversible with the blowing phase flow-field identical but opposite of the suction phase.

In [9] the different reference velocity is proposed. The U_0 velocity is based on the "stroke length" L_0 of the actuator:

$$L_0 = \int_0^{T/2} u_0(t)\, dt, \quad U_0 = L_0 f, \qquad \{2\}$$

where $u_0(t)$ is the centreline slot velocity as a function of time (using the cross-stream average), t=0 is the start of the blowing stroke, T=1/f is the oscillation period, and L_0 (stroke length) is the length of the slug of fluid pushed from the slot during the blowing stroke. Then, the corresponding Reynolds number is:

$$Re_0 = \frac{U_0\, h}{\nu}. \qquad \{3\}$$

Note that U_0 is neither the time average of u_0 over a cycle T nor its time average over a time T/2. Instead, U_0 is essentially the downstream-directed velocity, which occurs only during the blowing half of the cycle, averaged over the full cycle.

Stroke length nondimensioned using the orifice size could be an important parameter. Also For rectangular orifice, its aspect ratio could play an important role.

The different Reynolds number based on an impulse I_0, is defined in [12]:

$$Re_{I_0} = \frac{I_0}{\mu h}. \qquad \{4\}$$

Impulse I_0, i.e. the momentum associated with the discharge could be defined as follows:

$$I_0 = \rho \int_0^{T/2} \int_A u_0^2(\alpha, t)\, dA dt\,, \qquad \{5\}$$

where ρ is fluid density and A is an orifice area.

The unsteady effect are best described by a Stokes number:

$$St = \frac{\omega h^2}{\nu}, \qquad \{6\}$$

where ω is the operating frequency. The Stokes number compares the thickness of the unsteady boundary layer in the orifice ($\delta^2 \sim \nu/\omega$) to the size of the orifice, h. If the St is large, the orifice is not strongly influenced by viscous effects, while if St is small, the orifice is strongly viscous, and the jet can choke on the unsteady boundary layer.

The Reynolds and Stokes number could be combined to form a Strouhal number:

$$Sh = \frac{St}{Re} = \frac{\omega h}{U}, \qquad \{7\}$$

this compares the operating frequency to the typical time taken by a fluid element to advect through the orifice zone. Large Sh indicate that the actuator cycles several times before a fluid element manages to passes through the orifice region, while small Sh indicate that the fluid elements pass through the orifice in one cycle.

Another useful frequency characterizing parameter is dimensionless frequency F^+, which is measure of the total impulse per unit time and thus may be used as a parameter that characterizes different jets according to their strength:

$$F^+ = \frac{f I_0}{\rho \nu^2} \qquad \{8\}$$

The characterization of the formation parameters of the jet is simplified when the jet is driven time-harmonically, and the formation parameters depend primarily on the frequency and amplitude of the driving mechanism (e.g., diaphragm or piston motion) and cannot be varied independently.

4. Isolated Synthetic Jet

An isolated synthetic jet in the absence of a cross flow is produced by the interactions of a train of vortices that are typically formed by alternating momentary ejection and suction of fluid across an orifice such that the net mass flux is zero. Whereas the nominally axisymmetric (or two-dimensional) flow during the suction stroke may be thought of as similar to the flow induced by a sink that is coincident with the jet orifice, the flow during the ejection stroke is primarily confined to a finite narrow domain in the vicinity of the jet centreline.

Detailed description of a synthetic jet formation is given e.g. in [12].

4.1. Jet Formation

As mentioned above, generation process of a synthetic jet consists of two phases: blowing or ejection and suction.

During the ejection phase, the flow separates at the sharp edges of the orifice and forms a vortex sheet that typically rolls into a vortex (vortex rings or vortex pairs for circular or two-dimensional orifices, respectively) that moves away from the orifice under its own self-induced velocity. The degree of interaction between the vortex and the reversed flow that is induced near the orifice by suction of makeup fluid when the pressure drop across the orifice is reversed depends on the impulse of the vortex and its distance from the orifice.

During the suction stroke, a counter-rotating vortex pair is formed at the inner edges of the orifice, impinges on the opposite wall, and dissipates near the centre of the cavity (apparently owing to the injection of opposite sense vorticity from the wall boundary layer) before the next ejection cycle begins. For a given Reynolds number, the strength of the vortex pairs that are produced on both sides of the orifice appears to increase with decreased cavity height.

A Schlieren image in Figure 4 shows a vortex pair that is formed near the orifice as well as the outline of a turbulent jet farther downstream. Although the vortex pair and the remainder of the ejected fluid appear to be laminar after the rollup is completed, the cores of the vortex pairs become unstable and begin to break down to small-scale motions at the beginning of the suction phase. The onset of small-scale transition appears to take place near the front stagnation point of the vortex pair where the strain rates are high. Based on the Schlieren visualization, the transition process seems to proceed toward the rear of the vortex and ultimately progresses through the fluid stem behind it.

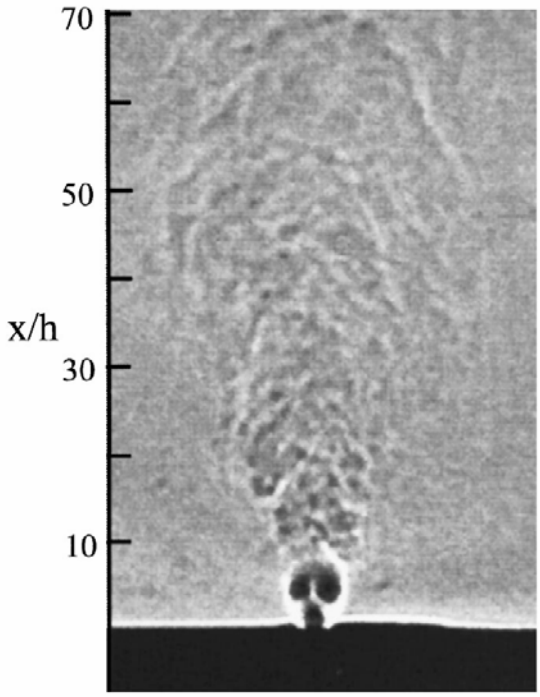

Fig.4 – Schlieren image of planar synthetic jet

4.2.Near-Field Evolution

In addition to the time-averaged centreline velocity $U_{cl}(x)$, and the celerity $U_c(x)$ of the vortex pair, the evolution of the jet near the exit plane may also be characterized by the magnitude of the phase-averaged residual centreline velocity between successive vortices at a given streamwise location – the residual offset velocity $u_{os}(x)$:

$$u_{os}(x) = \min\left(\left\langle u(t/T, x)\right\rangle\right) \qquad \{9\}$$

This velocity is, in part, a measure of the time-invariant velocity of fluid that is entrained into the jet column by the suction flow that is induced at the orifice. Figure 5 shows the streamwise variation of $U_c(x)$, $u_{os}(x)$ and $U_{cl}(x)$ in the near field (for $Re_0 = 18.124$) and shows that both the celerity and the centreline velocity decrease substantially during transition to turbulence (around $x/h = 7$). The celerity and the offset velocity change again at $x/h \approx 10$ and ultimately merge with the mean velocity at $x/h > 20$.

The time-periodic reversal in flow direction along the jet centreline during the blowing and suction strokes leads to the time-periodic appearance of a stagnation (saddle) point on the centreline located between the recent vortex and the jet exit plane that moves along the centreline during the suction stroke. The presence of a stagnation point in phase-averaged streamline maps of a two-dimensional jet (Figure 3) that are computed from PIV data. The stagnation point is located at $x/h = 5$ and the stagnation streamlines on both sides of the stagnation point separate between the flow that is driven by the ejection stroke and the suction flow towards the jet orifice. The latter is restricted to the domain that is also bounded by the

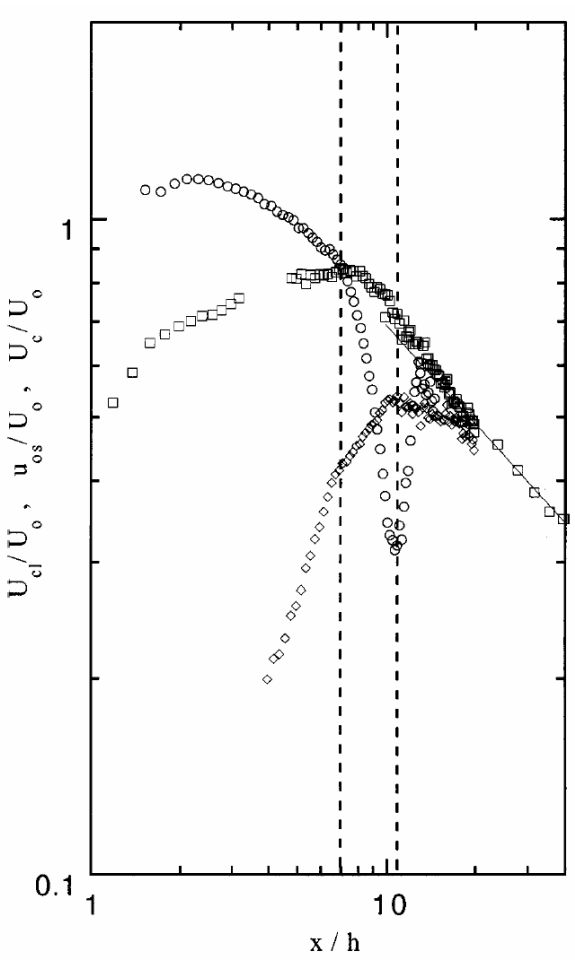

Fig.5 – Mean centreline velocity (□), celerity (○) and offset velocity (◊)

exit plane of the jet and is nominally symmetric with respect to the jet centreline. The streamline map also shows that the flow downstream of the branches of the stagnation point on both sides of the centreline is directed toward the jet orifice and then turns around in the streamwise direction near the cross-stream edges of the jet. In [35] there is also noted that the symmetry of the flow that is moved toward the orifice during the suction stroke can be altered on either side of the jet centreline by extending one of the edges of the jet orifice in the downstream direction thus restricting the suction flow on that side and increasing the flow rate on the opposite side of the jet orifice. The length of the extension is of the order of the orifice width. As shown by the authors, the ability to control the symmetry of the suction flow plays an important role in the vectoring of conventional jets by synthetic jet actuators.

4.3.Far Field Evolution

The fundamental works on a synthetic jet physics show that although cross-stream distributions of the time-averaged streamwise and cross-stream velocity components and the corresponding rms velocity fluctuations appear to collapse in the usual similarity coordinates, the streamwise scaling of other variables (e.g., the centreline velocity, jet width, volume flow rate, etc.) do not match corresponding scaling for conventional jets. For example, whereas the width b of a two-dimensional synthetic jet varies like $x^{0.88}$ ($b \sim x$ for a conventional two-dimensional jet), the longitudinal derivation db/dx is almost twice as large as in conventional jets. Furthermore, even though the streamwise variation of the jet volume flow rate dQ/dx is smaller than in conventional jets, the net entrained volume flow rate of the synthetic jet within the domain $x/b < 80$ is nearly $4Q_0$ ($Q_0 = U_0 b$) and substantially larger than for conventional jets. This departure from conventional self-similarity is apparently associated with a streamwise decrease in the jet's momentum flux, which is typically assumed to be an invariant of the flow for conventional self-similar two-dimensional jets. This decrease in the momentum flux of synthetic jets is a result of the adverse streamwise pressure gradient near the jet orifice that is imposed by the suction cycle of the actuator and is manifested by a time-averaged static pressure, which is lower than the ambient.

Velocity spectra of synthetic jets are characterized by the rapid streamwise attenuation of spectral components above the formation frequency of the jet thus indicating strong mixing and dissipation within the jet and reduction in the total turbulent kinetic energy. Power spectra of the centreline velocity of a two-dimensional jet are shown in Figures 6a-c (measured at $x/b = 5.9$, 19.7, and 177.2, respectively). Near the jet exit plane (Figure 6a), the spectrum is dominated by the formation frequency and its higher harmonics (hot-wire rectification within this domain also adds higher harmonics), whereas the spectral distribution below the fundamental frequency is virtually featureless. The harmonics of the formation frequency are rapidly attenuated with downstream distance and by $x/b = 19.7$; only the fundamental and its first harmonics are present and there is a significant increase in the magnitude of the spectral band below the formation frequency. Therefore, following the time-harmonic formation of the discrete vortex pairs, energy is transferred from these primary ("large-scale") eddies, which coalesce to form the jet, both to the mean flow and to smaller scales at which dissipation ultimately takes place. It is remarkable that the spectral band below the formation frequency (with the exception of a weak spectral band around 10 Hz) remains featureless and shows no evidence of sub-harmonics of the formation frequency (and thus of pairing interactions between the jet vortices). Subharmonic frequencies were present in the DNS of a two-dimensional synthetic jet [7] where the evidence of vortex pairing at low Reynolds numbers based on the jet peak velocity is presented. However, these authors noted that the pairing interactions might have been the consequence of the closed streamwise-periodic simulation domain.

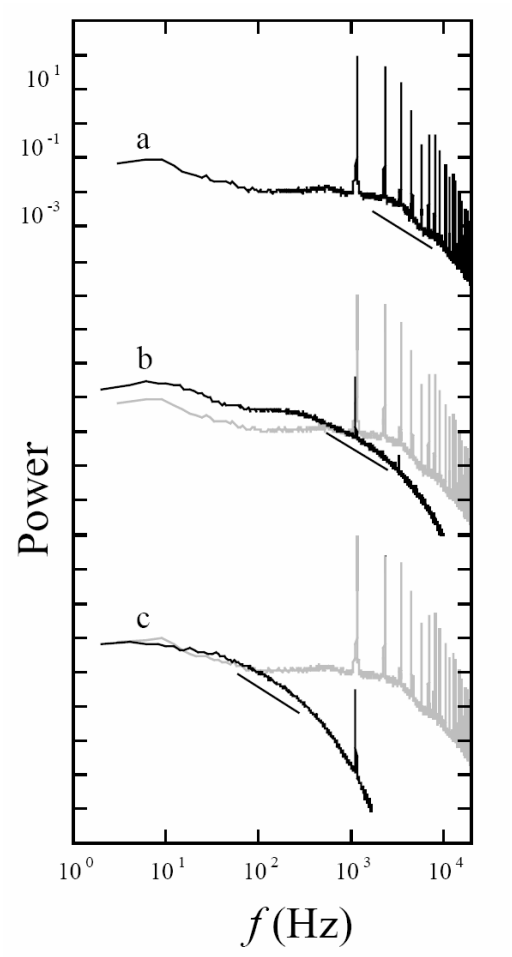

Fig.6 – Power spectra of the centreline velocity, $x/b = 5.9$ (a), 19.7 (b), 177.2 (c)

A striking feature of the velocity spectra in Figures 6b and c is the rapid streamwise attenuation of high spectral components indicating strong dissipation within the synthetic jet and a reduction in the total turbulent kinetic energy. By $x/b = 177$ (Figure 6c), the nominal magnitude of the band $f < 100$ Hz is comparable to the corresponding band near the jet exit plane (suggesting energy transfer to the smaller scales) and at the same time, the "rollover" frequency moves towards lower frequencies. The spectral distributions in Figures 6b and c also include a relatively narrow frequency band having a slope of approximately -5/3, suggesting the existence of an inertial subrange, which is limited by the low Reynolds number of the flow. It is important that because the characteristic local centreline velocity decreases with downstream distance, the spectral peak at the formation frequency actually shifts toward higher wave numbers where the dissipation ultimately takes place.

5. Comparison with Continuous Jet

In [36] description of experiments comparing conventional continuous jet, pulsed jet and synthetic jet is given using the unique experimental facility allowing keeping the value of Reynolds number of about 2000 for all cases.

In the far-field, synthetic jets bear much resemblance to continuous jets in that the self-similar velocity profiles are identical. However, in the near field, synthetic jets are dominated by vortex pairs that entrain more fluid than do continuous jet columns. Therefore, synthetic jets grow more rapidly, both in terms of jet width and volume flux, than do continuous jets.

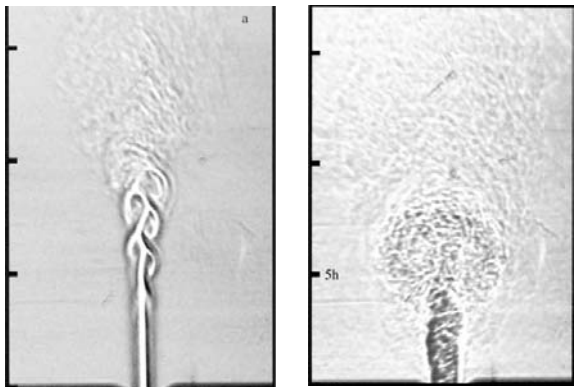

Fig.7 – Comparison of continuous and synthetic jet at Re_0=2200

In Figure 7 the Schleiren photographs of conventional continuous jet and synthetic jet in comparable condition are shown. Substantial differences in the jet dimensions as well as flow-field structure are evident. Whereas the conventional jet forms system of eddy structures, in the case of synthetic jet only a pair of vortices is distinct. Much more intensive entrainment process in synthetic jet flow-field results in wider jet flow. According to experimental results published in [34], the streamwise decrease of the mean centreline velocity of the synthetic jet is somewhat higher: $\sim x^{-0.58}$, while $\sim x^{-0.50}$ for conventional jet. The streamwise increase of the jet width and volume flow rate is lower for the synthetic jet: $\sim x^{0.88}$ and $\sim x^{0.33}$, respectively, the conventional jet exhibits $\sim x^{1}$ and $\sim x^{0.5}$.

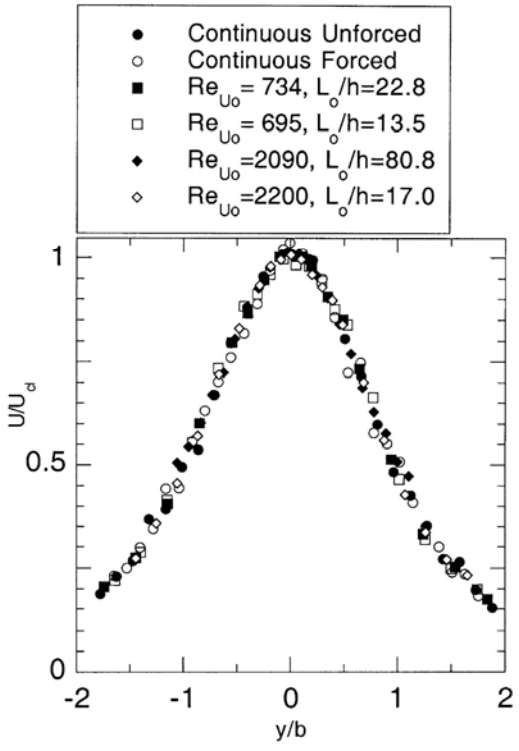

Fig.8 – Self-similar velocity profiles

In Figure 8 the nondimensional velocity profiles for corresponding continuous conventional jet, periodically forced conventional jet and various synthetic jets are shown measured in the downstream station at which $U_{cl} = 0.5U_0$. The velocity profiles of each jet, normalized in the usual fashion using local values of the jet width and the maximum time-averaged velocity U_{cl}, collapse for all cases. At these downstream distances, it appears that the time-averaged features of the jets exhibit little or no memory of how the jets were generated. Profiles of synthetic jets with much smaller U_0 values also collapse to the same shape, indicating that the use of local variables for normalization renders this measurement insensitive to U_0.

In the far field, the synthetic jet is

similar to conventional 2D jets in that cross-stream distributions of the time-averaged velocity and the corresponding rms fluctuations appear to collapse when plotted in the usual similarity coordinates. This departure from conventional self-similarity is consistent with the streamwise decrease in the jet's momentum flux as a result of an adverse streamwise pressure gradient near its orifice. While for conventional self-similar 2D jets the momentum flux is presumably an invariant of the motion, the momentum flux of synthetic jets decreases with streamwise distance as a result of an adverse streamwise pressure gradient near the jet orifice that is associated with the suction cycle of the actuator and an induced mean static pressure which is lower than the ambient.

The fact that the forced jet is wider while its volume flux is identical to that of the unforced jet is consistent with the behaviour of the centreline mean velocity shown in Figure 9. The velocity begins to decrease from the exit value after the jet becomes turbulent (near $x/h = 5$ for the forced jet; $x/h = 10$ for the unforced jet). Therefore, the forcing results in a jet that is wider and slower, but of the same volume flux.

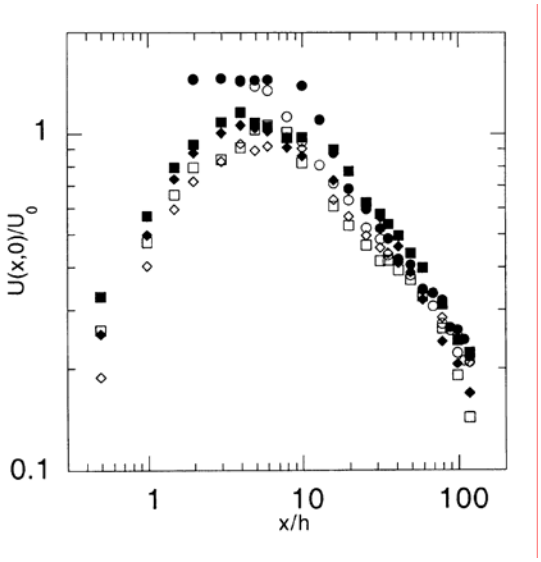

Fig.9 – Time-averaged centreline velocity vs downstream distance. (symbols as in Fig.8)

The mean velocity of synthetic jets at the exit is zero, and Figure 9 shows that it rises to a level very near U_0. Note that the value is higher for round synthetic jets. Before the –1/2 power-law decay typical of plane jets begins. Despite the range of Reynolds number and dimensionless stroke length in the data of Figure 9, the centreline velocities behave essentially the same in every case. In the near field, the mean centreline velocity for the synthetic jets consistently lies below that of the continuous jets, indicating that the synthetic jets are wider and slower than matched continuous jets.

6. Synthetic Jet Interactions

A synthetic jet is to be used for control of various types of shear flows. To study insight of the controlling mechanism, the interaction of a synthetic jet with a typical shear flow – boundary layer is a good and logical starting point.

The interaction of synthetic jets with an external cross flow over the surface in which they are mounted can displace the local streamlines and induce an apparent or virtual change in the shape of the surface and thereby effecting flow changes on length scales that are one to two orders of magnitude larger than the characteristic scale of the jets. This control approach emphasizes an actuation frequency that is high enough so that the interaction domain between the actuator and the cross flow is virtually invariant on the global time scale of the flow and therefore global effects such as changes in aerodynamic forces are effectively decoupled from the operating frequency of the actuators.

Interaction of a synthetic jet and turbulent boundary layer was studied in [33] and [28]. The interaction between the synthetic jet and the boundary layer is strongly influenced by the orientation of the synthetic jet orifice. The blockage of the flow is significant in the near field and the flow downstream can be interpreted broadly as the wake of this obstruction, although

there is evidence to suggest that this wake contains a distinct structure. The mean velocity profiles suggest that high momentum fluid is swept toward the wall along the interaction centreline and away from the wall off centre. Moreover, the velocity profiles are similar to those measured in a continuous jet in crossflow. In the near-wall region, the wall-jet character of profiles has been observed. The observed trends in the integral parameters suggest that synthetic jet is decoupled from the turbulent flow in the boundary layer and, as its trajectory carries it beyond the boundary-layer edge, the boundary layer assumes characteristics consistent with its state before the interaction. The displacement and momentum thickness both increase monotonically over the streamwise extend of the measurement domain, whereas the shape factor remains unchanged.

The simulations show that the presence of the crossflow results in a significantly different flow as evidenced by the dynamics of the vortex structures produced by the jet and the jet velocity profiles. A systematic framework has been put forth for characterizing the jet in terms of the moments of the jet profiles. In addition to the moments, the simulations also indicate that skewness might be an important characteristic of the jet profile. Separate analysis of the suction and blowing strokes is also found to be useful since it reveals distinctly different jet behaviour during these two phases for cases where there is an external crossflow. Concerning the virtual aero-shaping effect it was found that large mean recirculation bubbles are formed in the external boundary layer only if the jet velocity is significantly higher than the crossflow velocity.

7. Adjacent Synthetic Jets

Tangential injection i.e. wall jet is a preferred way of a boundary layer control. To adopt this type of boundary layer excitation using synthetic jets actuators there are two ways. Firstly, the jet orifice could be inclined with respect of the wall surface. The second possibility is force the jet to bend.

This could be achieved by adjacent jets technique by placing two synthetic jets in close proximity. The resultant jet can be effectively manipulated by modifying the formation and evolution of the vortex pairs of each jet by varying the amplitudes or the relative phase of the driving waveforms. In particular, phase variation between the driving signals effectively changes the relative timing of the rollup of the adjacent vortex pairs and thus leads to strong vortex interactions that alter the trajectories of the vortex pairs and the direction of the ensuing jet. Figure 10 shows a Schlieren image of the jets and demonstrates the effect of phase variation between two driving signals having the same frequency and amplitude. When the two jets are in phase Figure 10 (a), the inner vortices of each vortex pair cancel each other, resulting in a single, larger synthetic jet. When one of the jets is leading in phase, the interaction between the adjacent vortex pairs, which is also affected by the suction flow, alters their ultimate trajectories and the merged jet is vectored towards the leading jet. When the jet on the right is leading in phase by 60°, the merged jet is vectored to the right (case b) and when the phase angle is 150° (case c), the merged jet becomes almost attached to the exit plane.

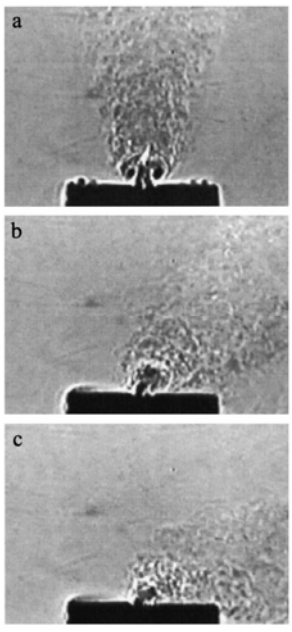

Fig.10 – Adjacent synthetic jets, phase shift
a) 0°, b) 60°, c) 150°

8. Synthetic Jet Actuators

Synthetic jets are typically formed by imposing a time-periodic alternating pressure drop across an orifice. This general task could be accomplished by various ways e.g. by acoustic waves or by the motion of a piston or a diaphragm in a cavity. However, in [15] have been shown that the cavity presence is not necessary.

Recent investigations have employed a variety of jet drivers including piezolectrically driven diaphragms, electromagnetically driven pistons and acoustically driven cavities. Newly, high power synthetic jets generators using combustion-powered actuator concept are extensively tested. Those generators produce high frequency periodical plasma jets, operating frequency is controlled by a spark ignition and refill timing. Frequency over 100Hz have been achieved up to now, however piezolectrically driven diaphragms could work at frequencies of order kHz.

In spite of the fact, that the synthetic jet outside the actuator is nearly not affected by acoustics, inside the actuator the acoustic effects are predominant. A sufficiently accurate mathematical model of a synthetic jet actuator could be constructed only in all its significant features are taken into account. Both acoustical features (Helmholtz resonance of the cavity) and structure features (resonance of the moving boundary – membrane or piston) should be taken into account. This results into a coupled dynamical system at least of fourth order, which is characterized by two resonances (details see e.g. [9], [10] or [41]). However, functionality of a synthetic jet actuator strongly depend on several design details as shape of cavity corners and edges, which could be taken into account only by complex CFD modelling or by experimental verification.

One of the major advances in flow control is the emergence of Micro Electro Mechanical Systems (MEMS) technology, which employs the methods developed for the fabrication of silicon chips to construct very small-scale mechanical devices. The significance of micromachine technology is that it makes it possible to provide mechanical parts of micron size, fabricated in large quantities, and integrable with electronics. Miniaturization to this scale is necessary for both sensors and actuators for successful feedback control of turbulence due to the very small scales of the coherent structures in high Reynolds number flows of engineering interest. Miniaturized actuators also simplify the integration of the control system with the overall structure or subsystem. MEMS fabrication processes provide not only miniaturization, but also modular integration of sensors, actuators, and electronics and the affordability enabled by batch processing. However, micro devices for active flow control do not obviate the role of meso-devices in flow control technologies.

9. Flow Control

The intent of flow control may be to delay/advance transition, to suppress/enhance turbulence, or to prevent/promote separation. The resulting benefits include drag reduction, lift enhancement, mixing augmentation, heat transfer enhancement, and flow-induced noise suppression. The objectives of flow control may be interrelated, leading to potential conflicts as the achievement of one particular goal may adversely affect another goal. For example, consider an aircraft wing for which the performance is measured by the improvement in lift-to-drag ratio. Promoting transition will lead to a turbulent boundary layer that is more resistant to separation and increased lift can be obtained at higher angle of incidence. The viscous or skin-friction drag for a laminar boundary layer can be an order of magnitude smaller than for a turbulent boundary layer. However, a laminar boundary layer is more prone to separation resulting in a loss in lift and an increase in form drag. The design trade-offs of a

particular method of control must carefully be evaluated and compromises are often necessary to reach a particular design goal.

Classification of flow control methods is based on energy expenditure and the control loop involved. Flow control involves passive or active devices that have a beneficial change on the flow field. A considerable amount of research has been performed using passive methods of flow control, which modify a flow without external energy expenditure. Passive techniques include geometric shaping to manipulate the pressure gradient, the use of fixed mechanical vortex generators for separation control, and placement of longitudinal grooves or riblets on a surface to reduce drag. Recent review of passive flow control including a detailed historical perspective on flow control is also given in [8]. During the last decade, emphasis has been on the development of active control methods in which energy, or auxiliary power, is introduced into the flow. Active control schemes can be divided into predetermined or interactive methods. A predetermined method of control involves the introduction of steady or unsteady energy inputs without consideration for the state of the flow field. Examples of predetermined active flow control include jet vectoring or post-stall lift enhancement and form drag reduction using synthetic jets actuators. Predetermined open-loop control schemes can be very effective in modifying the flow field.

In interactive methods of flow control, the power input to the actuator (controller) is continuously adjusted based on some form of measurement element (sensor). The control loop for interactive control can be either a feedforward (open) or feedback (closed) loop. In the feedforward control loop, the sensor is placed upstream of the actuator. Therefore the measured flow field parameter and the controlled flow field parameter will differ as flow structures convect over stationary sensors and actuators.

The utility of synthetic jets for flow control was demonstrated in the vectoring of conventional jets in the absence of extended control surfaces [27]. Since then, this approach to flow control has been adopted in a number of other applications, including the modification of the aerodynamic characteristics of bluff bodies, control of lift and drag on airfoils, reduction of skin friction of a flat plate boundary layer, mixing in circular jets, control of internal flow separation and control of cavity oscillations.

9.1. Separation Control

Active manipulation of separated flows with aim of complete or partial flow reattachment is in the centre of attention of many researchers during a few last decades. Reattachment of a separated boundary layer is affected by exploiting the receptivity of the separating shear layer to external excitation affecting evolution of vortical structures and their interactions with the body surface. Active flow control schemes have employed a variety of actuation techniques including external acoustic excitation, internal acoustic excitation, surface-mounted vibrating mechanical flaps and steady and unsteady blowing or bleeding.

An important parameter of the separation control process is the characteristic time scale of the actuation. Basically, there are two different concepts. Several investigations of the suppression of flow separation on airfoils, for example, have emphasized actuation frequencies that can couple directly to the instability mechanisms of the separating shear layer F^+ in order to effect a Coanda-like reattachment. This approach relies explicitly on the narrow-band receptivity of the separating shear layer to a control input that is effective within a limited spatial domain typically immediately upstream of separation, where the excitation is applied at a frequency that is of the order of the unstable frequency of the base flow such that the excitation period nominally scales with the time of flight over the length of the reattached flow. In contrast to this, in [1] there is demonstrated the utility of synthetic jet actuators for

suppression of separation at moderate Reynolds numbers (order of 10^6) using reduced actuation frequencies F^+ that are at least an order of magnitude higher than the characteristic (e.g., shedding) frequency of the airfoil. This approach emphasizes an actuation frequency that is high enough so that the interaction domain between the actuator and the cross flow is virtually invariant on the global time scale of the flow, and therefore, global effects such as changes in aerodynamic forces are effectively decoupled from the operating frequency of the actuators. At the same time, the broader control bandwidth can also be used to augment the quasi-steady aerodynamic forces by exploiting a prescribed unsteadiness of the separated flow domain using a temporally modulated actuation input to control the rate of vorticity shedding into the wake.

The total (mean and oscillatory) momentum coefficient could be defined as a ratio of the momentum added to tat in the free-stream:

$$C_\mu = \frac{\rho_j U_j^2 h}{1/2\,\rho_\infty U_\infty^2 c} \qquad \{10\}$$

Where ρ_j and U_j are fluid density and velocity of the jet fluid respectively, ρ_j and U_j are the same quantities related to outer flow, h is the jet orifice width, c is a typical dimension of the body (e.g. chord or diameter).

The value of the momentum coefficient for effective separation flow control could be within the range $0.01\% < C_\mu < 3\%$. A wide range of data showed conclusively that excitation is much more effective and efficient than steady blowing. Moreover, for aerodynamically inefficient bodies, excitation could bring large increase in lift and/or reduction in drag.

As an example the results obtained in study [11] are presented here. Figure 11 shows the visualized flow over the wing, at an angle of attack of 20 degrees, without (top) and with (bottom) synthetic jet actuation. Without the synthetic jet actuation, the flow separates very close to the leading edge and the wing is in the post-stall region. With the synthetic jet actuation, the flow remains attached over about 70% of the wing chord.

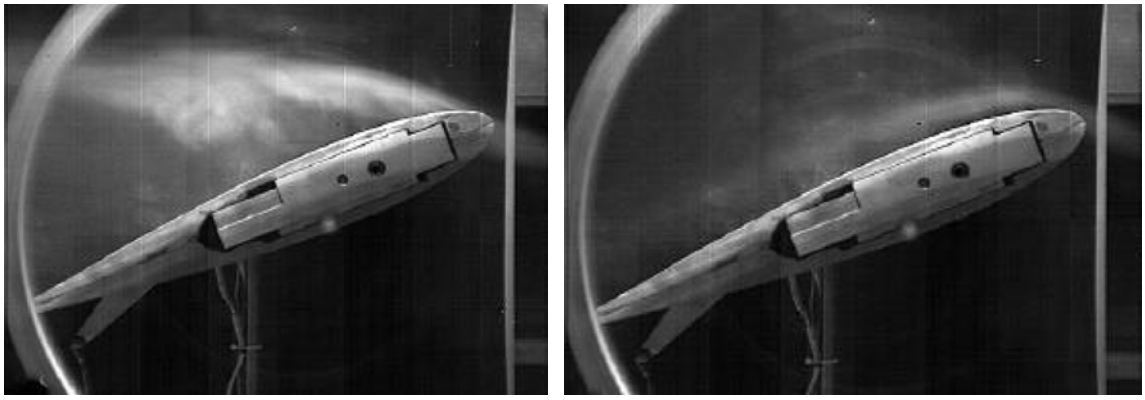

Fig.11 – Flow visualization over a wing without (left) and with (right) synthetic jet actuation

9.2. Virtual Aeroshaping

Usage of the synthetic jets for active control of separation has been studied quite extensively. It has been demonstrated that synthetic jets can indeed reduce the extent of separation over bluff as well as streamlined bodies. Despite these successful demonstrations, it is fair to state that the physical mechanisms through which synthetic jets accomplish this reduction in separation are not completely understood.

Separation over an airfoil is typically an unsteady process that is accompanied by the formation of large-scale vortex structures in the separated shear layer. The characteristic frequency of formation of these vortex structures is $O(U_\infty/L_s)$ where L_s is the length of the separation zone and U_∞ the free-stream velocity. There is broad consensus that synthetic jets operating in this frequency range tend to promote and amplify the formation of the vortex structures in the separation region. These vortex structures entrain high momentum free-stream fluid into the separated flow region and this promotes the early reattachment of the separated boundary layer. In the case where the boundary layer is laminar at separation, synthetic jets operating at much higher frequencies could also lead to earlier transition in the boundary layer. Since a turbulent boundary layer is more resistant to separation, earlier transition to turbulence can delay the separation.

Both of the above mechanisms are not unique to synthetic jets but have indeed been well known in the context of active separation control for quite some time. In addition to these two mechanisms, the unique characteristics of the flow produced by a synthetic jet interacting with a crossflow have also led researchers to suggest other flow features/mechanisms that might play a role in separation reduction in flows where these actuators are employed. One of these is the so-called ‘‘virtual aeroshaping’’ effect. It has been suggested that due to the zero net mass flux constraint, synthetic jets are capable of forming recirculation bubbles in the mean external flow and these can be significantly larger in size than the jet orifice/slot size. An example of 2D simulation (from [21]) is shown in Figure 12. It has further been suggested that these large bubbles effectively modify the shape of the body, consequently altering the pressure gradient and the extent of separation. This capability of synthetic jets is extremely desirable since it would potentially allow for ‘‘on-demand’’ virtual morphing of the wing section. The effect of virtual shape change is indicated by a localized increase of surface pressure in the neighbourhood of synthetic jet actuation. That causes a negative lift to the airfoil with an upper surface actuation. When actuation is applied near the airfoil leading edge, it appears that the stagnation line is shifted inducing an effect similar to that caused by a small angle of attack to produce an overall lift change.

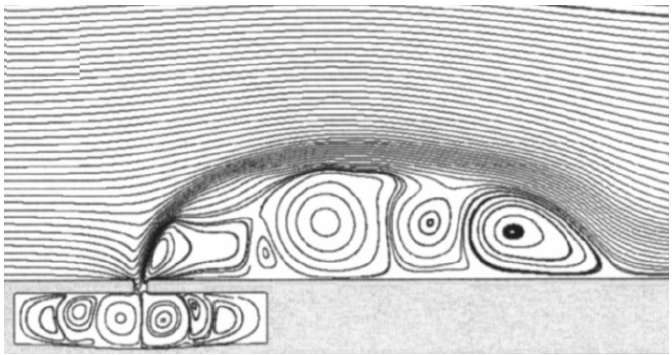

Fig.12 – Streamlines of a synthetic jet – crossflow interaction (crossflow from left)

The interaction of a synthetic jet (or jet arrays) with an external cross flow over the surface in which they are mounted can displace the local streamlines and induce an apparent or virtual change in the shape of the surface and is, therefore, of considerable interest for flow control applications. The control of aerodynamic flows by modifying the apparent shape of aerosurfaces in order to prescribe the streamwise pressure distribution and thereby influence their aerodynamic performance is not new and was addressed in a several investigations in the 1940s and 1950s. In a recent investigation of the evolution of synthetic jets on the surface of a two-dimensional cylinder, in [14] there were demonstrated that when the jets are operated on a timescale that is well below the characteristic timescale of the base flow, the formation of a quasi-steady interaction domain near the surface is accompanied by a more favourable pressure gradient. As a result, the surface boundary layer downstream of this domain becomes

thinner allowing the flow to overcome stronger adverse pressure gradients and therefore delaying (or altogether suppressing) flow separation.

Some fundamental features of virtual aerodynamic modification of bluff bodies have been investigated in the flow around a circular cylinder in a uniform cross-stream. This base flow provides a unique opportunity to place the jet at various azimuthal positions having different local pressure gradients and to investigate its global effect on the flow field and the aerodynamic forces on the model. The interaction between the jets and the cross flow over the cylinder model were first investigated in a flow visualization study by Amitay et al. (referred in [12]) for a number of azimuthal jet positions (Figures 13a-d). Rotation of the cylinder around its axis varies the azimuthal jet location relative to the front stagnation point γ and the actuation level is characterized using the momentum coefficient C_μ (see {10}), where the typical dimension c is the cylinder diameter.

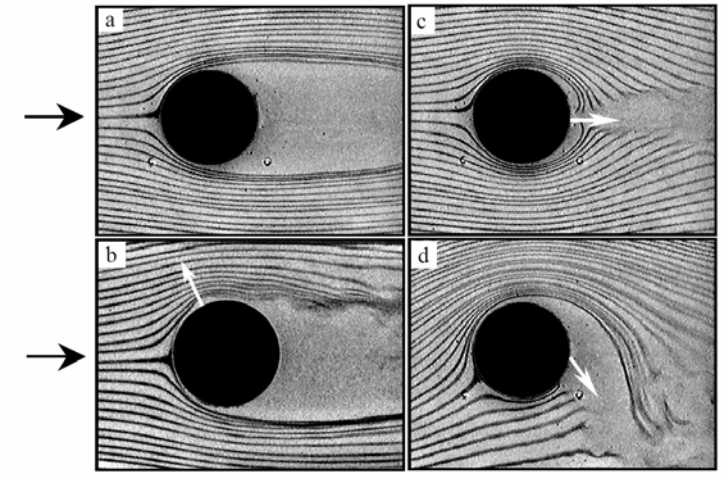

Fig.13 – Visualization of flow around a circular cylinder
a) baseline, b) actuated $\Phi = 0$, g = 60°, c) $\gamma = 120°$,

The baseline flow is shown for reference in Figure 13a and appears to separate at $\theta \sim 80°$. When the jets are placed at $\gamma = 60°$ (Figure 13b), and are operated in phase so that the combined C_μ is $O(10^{-3})$, the effect on the cross-flow is manifested by a relatively small local deformation of smoke streak-lines above the top surface of the cylinder. Although the changes in the external flow are somewhat subtle, it is apparent that the separation point on the top surface moves downstream and that the front stagnation point is displaced below the mean flow direction (i.e., towards the bottom of the cylinder). Other visualization images show that the cross stream symmetry of the cylinder wake can be substantially altered when the jets are placed in the azimuthal domain $100° < \gamma < 180°$ for increased levels of C_μ and can induce the formation of two uneven closed recirculating regions. When the jets are placed at $\gamma = 180°$ and C_μ is increased to $O(10^{-1})$ (Figure 7c), the external flow appears to be almost attached to the surface of the cylinder. Finally, in Figure 13d the jets are still placed at $\gamma = 180°$ but they are operated out of phase such that the bottom jet is leading by $2\pi/3$. Out-of-phase operation of adjacent synthetic jets results in vectoring of the combined jet towards the jet that is leading in phase. The vectoring of the jets results in downward deflection of the entire wake and a concomitant displacement of the front stagnation point, which is qualitatively similar to classical flow visualization snapshots of the flow around a spinning cylinder. The decrease and increase in the spacing between streaklines above and below the cylinder, respectively are indicative of a change in circulation and generation of lift.

9.3. Mixing Control

In [6] and [23] the utility of synthetic jet actuators for the modification and control of small-scale motions and mixing processes is investigated in the shear layer of a round jet. Mixing of the two jets – circular one in the centre and the other annular surrounding the first

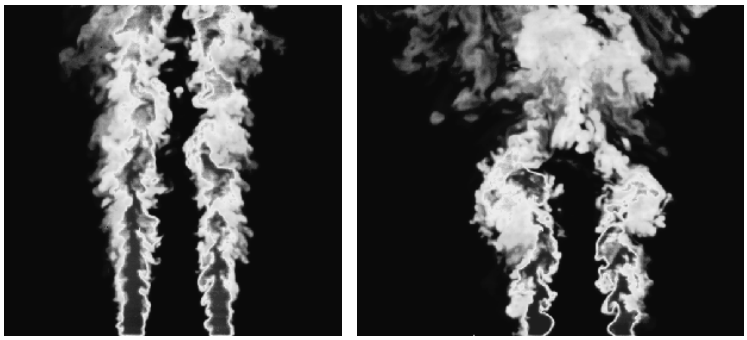

Fig.14 – Mixing of unforced (left) and forced (right) jet

one. Enhancement of mixing between an annular jet and both ambient air and an inner air jet is achieved with synthetic jets. A round turbulent air jet is instrumented with an azimuthal array of individually controlled synthetic jet actuators placed near the jet exit plane to effect direct small-scale excitation within the equilibrium range of the primary jet shear layer. The control jets can be directed either normal to the primary jet or parallel to its centreline. The excitation results in a substantial increase in the rms velocity fluctuations throughout the core of the primary jet and leads to the suppression of the "natural" Kelvin-Helmholtz instability of the jet shear layer. Azimuthally-periodic forcing distorts the jet cross section and appreciably lengthens the jet shear layer. Amplitude modulation of the excitation waveform enables temporal control of the large-scale structures within the flow, leading to substantial increases in spreading rate and entrainment of the primary jet. Actuators driven by sufficiently high-frequency signal can excite small scales in the flow, and large scales can also be excited by amplitude modulation of the actuators. Effect of forcing on mixing process is demonstrated in Figure 14.

In [7] the annular synthetic jet is used for mixing control of the stack jet plume. The synthetic jet is produced coaxially to the stack pipe. Interaction of the plume with coaxial synthetic jet issuing into a crossflow was studied. The resulting effect strongly depends on conditions of the interaction. Proper choice of the annular synthetic frequency and amplitude determines the resulting effect. Generally, an increasingly complex periodic 3D vortex structures are produced. However, if the synthetic jet velocity is near the laminar jet velocity, relaminarization of the plume take place. When the forcing velocity is near the peak in the cross-jet velocity, an abrupt transition in the vortex structure was observed. Finally, increasing of mixing process is achieved at high forcing amplitudes. Also a few effects interesting from the point of view good pollutant dispersion from the chimney have been observed. Firstly, the downwash is reduced or even eliminated by acting of the synthetic jet. The, average plume height increases with increased forcing amplitude.

9.4. Jet Vectoring

An effective method to vector a conventional jet has been discovered by Smith and Glezer and presented in [35]. A synthetic jet actuator is placed adjacent to the exit plane of a high aspect ratio rectangular primary jet as shown in Figure 15. The top Schlieren image shows the primary jet unforced. The bottom Schlieren image shows the synthetic jet is activated and the primary jet vectored toward the actuator at an angle of nearly 30°. The location of the synthetic jet actuator is also depicted. Schlieren visualizations of the flow with and without control are shown. The vectoring results from the synthetic jet drawing fluid from the primary jet conduit. The flow near the top of the duct accelerates, while the pressure along the top is reduced, resulting in a vertical pressure gradient in the duct.

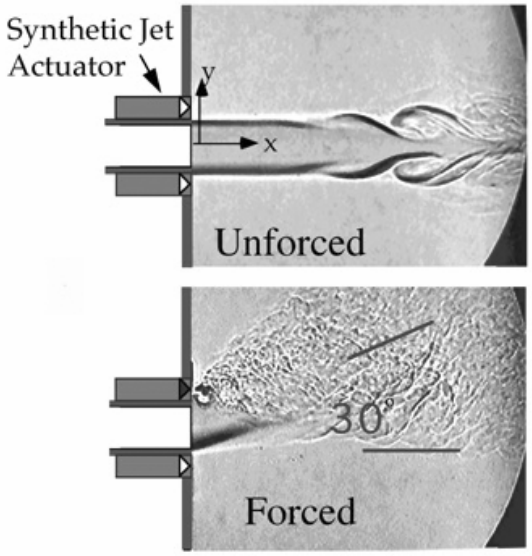

Fig.15 – Schlieren images of unforced and forced jet

(e.g. a diffuser or collar) that is balanced by a force on the primary jet conduit. For a synthetic jet of a given Reynolds number and duty cycle and fixed primary jet speed, the volume flow rate of primary jet fluid that is diverted into the synthetic jet depends on the driving frequency and, as discussed below, can be regulated by restricting the flow of entrained ambient fluid.

The proximity of the synthetic jet to the primary jet allows the two jets to interact such that during the suction stroke the synthetic jet draws some of its fluid from the primary jet. This interaction results in the formation of a low-pressure region between the two jets and the acceleration of the primary jet fluid near the upper conduit wall – see Figure 16. Then, the pressure field induced by the interaction between the jets leads to the turning of the flow inside the conduit upstream of the exit plane. The cross-stream momentum of the vectored primary jet balances a normal force on the conduit. The entrainment of primary jet fluid by the adjacent synthetic jet leads to alteration of the static pressure near the flow boundary and results in deflection of the primary jet toward the synthetic jet even in the absence of an extended control surface

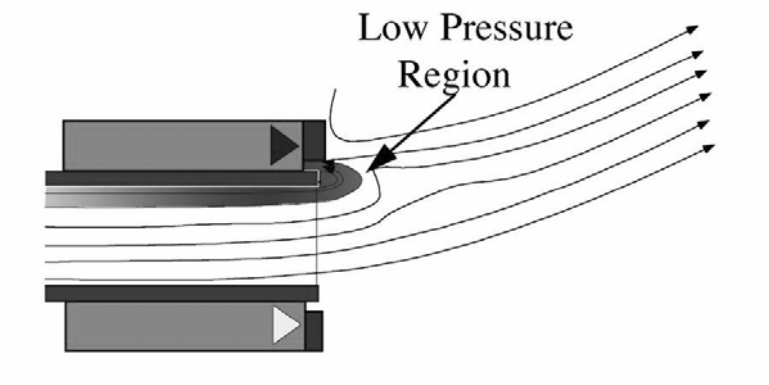

Fig.16 – Pressure distribution

9.5. Skin Friction Control

In interactive methods of flow control, the power input to the actuator (controller) is continuously adjusted based on some form of measurement element (sensor). The control loop for interactive control can be either a feed-forward (open) or feedback (closed) loop. In the feed-forward control loop, the sensor is placed upstream of the actuator. Therefore the measured flow field parameter and the controlled flow field parameter will differ as flow structures convect over stationary sensors and actuators.

The small-scale manipulation of the turbulent fluctuations is a challenging technological problem. In cases in which the control must interact with a specific set of turbulent fluctuations already present in the flow, such as random coherent structures, the effectiveness of an open-loop system is reduced. In the feedback control loop, a sensor is also placed downstream of the actuator to measure the controlled flow field parameter. The controlled variable is compared with the upstream reference variable. A feedback control law is utilized to control the energy introduced at the actuator. The interactive feedback control

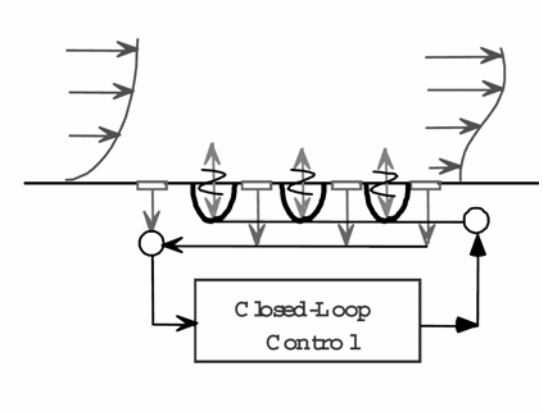

Fig.17 – Feedback control of skin friction

could be classified into four schemes based on the extent to which they are based on the governing flow equations: adaptive control, physical model-based, dynamical systems-based, and optimal control. A depiction of a closed-loop system is shown in Figure 17 for a boundary layer.

Until now predominantly results of mathematical modelling of the skin friction control have been published (see [8]), implementation this principle into experiments or even into the praxis represents itself a challenge to experimenters and engineers.

10. Conclusions

Much of the interest in synthetic jets stems from their potential utility for flow control applications, specifically control of the performance of aerodynamic surfaces through fluidic modification of their apparent aerodynamic shape. As shown in Section 3, the interaction domain between a synthetic jet and a cross flow over a solid surface can lead to a local displacement of the cross flow and thereby induce an "apparent" modification of the flow boundary and alter the local pressure and vorticity distributions. Earlier investigations have shown that these attributes may be exploited to modify or control the evolution of wall-bounded and free-shear flows (e.g., flow separation, jet vectoring, vortex flows, etc.) on scales that are one to two orders of magnitude larger than the characteristic length-scale of the synthetic jets themselves. Furthermore, active modification of the apparent shape of aerodynamic surfaces could enable the tailoring of the pressure gradient on existing aerodynamic surfaces to overcome effects of adverse pressure gradients and local separation, thereby enabling unconventional aerodynamic design approaches that are driven primarily by mission constraints (e.g., payload, stealth, volume, etc.).

11. Acknowledgement

It should be indicated, that this study has been carried out with the help of the project of the grant agency of the AS CR No.: A2076403 supported from the budged of the Czech Republic and the research project No.: K2076106.

12. References

[1] Amitay, M., Glezer, A., 1999, "Aerodynamic Flow Control of a Thick Airfoil Using Synthetic Jet Actuators, Proceedings of the 3rd ASME/JSME Joint Fluids Engineering Conference, July 18-22, 1999, San Francisco.

[2] Amitay, M.. Glezer A., 2002, "Controlled transients of flow reattachment over stalled airfoils", International Journal of Heat and Fluid Flow, 23, 2002, pp.690–699.

[3] Béra, J.-C., Michard, M., Sunyach, M., Comte-Bellot, G., 2000, "Changing lift and drag by jet oscillation: experiments on a circular cylinder with turbulent separation", Eur. J. Mech. B – Fluids, 19, 2000, pp.575–595.

[4] Chen, F.J., Beeler, G.B., 2002, "Virtual Shaping of a Two-dimensional NACA 0015 Airfoil Using Synthetic Jet Actuator", AIAA-2002-3273.

[5] Coustols, E, 1996, “Control of Turbulent Flows for Skin Friction Drag Reduction”, In: Control of Flow Instabilities and Unsteady Flows, Edited by G.E.A. Meier, G.H. Schnerr, Springer, pp.155-202.
[6] Davis, S.A., Glezer, A., 1999, “The Manipulation of Large- and Small-Scales in Coaxial Jets using Synthetic Jet Actuators,. AIAA Paper 2000-0403, 38th Aerospace Sciences Meeting, Reno, NV, 2000.
[7] Diep, J., Sigurdson, L., 2003, “Low Velocity Ratio Transverse Jets Influenced by Concentric Synthetic Jets”, In. Manipulation and Control of Jets in Crossflow, Edited by A.R. Karagozian, L. Cortelezzi, A. Soldati, Springer, pp.257-269.
[8] Gad-el-Hak, M., 2000, “Flow Control: Passive, Active, and Reactive Flow Management”, Cambridge University Press.
[9] Gallas, Q., Holman, R., Nishida, T., Carroll, B., Sherplak, M., Cattafesta, L., 2003, “Lumped Element Modeling of Piezoelectric-Driven Synthetic Jet Actuators”, AIAA Journal, vol.41, No.2, February 2003, pp.240-247.
[10] Gallas, Q., Wang, G., Papila, M., Sherplak, M., Cattafesta, L., 2003, “Optimization of Synthetic Jet Actuators”, AIAA 2003-0635.
[11] Gilarranz, J.L., Traub, L.W., Rediniotis, O.K., 2002, “Characterization of a compact, high power synthetic jet actuator for flow separation control”, AIAA-2002-0127.
[12] Glezer, A., Amitay, M., 2002, “Synthetic jets”, Annu, Rev. Fluid Mech., **34**, pp.503-529.
[13] Holman, R., Gallas, Q., Carroll, B., Cattafesta, L., 2003, “Interaction of Adjacent Synthetic Jets in an Airfoil Separation Control Application“, 33rd AIAA Fluid Dynamics Conference & Exhibit, 23-26 June 2003 / Orlando, FL, AIAA 2003-3709.
[14] Honohan, A.M., Amitay, M., Glezer, A., 2000, “Aerodynamic Control Using Synthetic Jets”, AIAA-2000-2401.
[15] James, R.D., Jacobs, J.W., Glezer, A., 1996, “A Round Turbulent Jet Produced by an Oscillating Diaphragm”, Physics of fluids, volume 8, number 9, September 1996, pp.2484-2495.
[16] Lee, C.Y., Goldstein, D.B., 2000, “Two-dimensional synthetic jet simulation”, AIAA Fluids 2000, 2000-0406.
[17] Lee, C.Y., Goldstein, D.B., 2002, “ Simulation of MEMS Suction and Blowing for Turbulent Boundary Layer Control”, AIAA,2002-2831, 1st Flow Control Conference, 24-26 June 2002, St.Louis.
[18] Lee, C., Hong, G., Ha, Q.P., Mallison, S.G., 2003, “A piezoelectrically actuated micro synthetic jet for active flow control”, Sensors and Actuators A 108, pp.168-174.
[19] Lighthill, J., 1978, “Acoustic Streaming”, Journal of Sound and Vibration, vol.61, No.3, pp.391-418.
[20] Lorber, P., McCormick, D., Anderson, T., Wake, B., MacMartin, D., Pollack, M., Corke, T., Breuer, K., 2000, “Rotorcraft Retreating Blade Stall Control”, AIAA 2000-2475.
[21] Mittal, R., 2002, “On the virtual aeroshaping effect of synthetic jets“, Physics of Fluids, Volume 14, Number 4, April 2002, 1533-1536.
[22] Rathnasingham, R., Breuer, K.S., 1997, “Coupled Fluid-Structural Characteristics of Actuators for Flow Control”, AIAA Journal, vol.35, No.5, pp.832-837.
[23] Ritchie, B.D., Mujumdar, D.R. and Seitzman, J.M., 2000, “Mixing in Coaxial Jets Using Synthetic Jet Actuators”, AIAA 2000-0404.
[24] Ravindran, S.S., 1999, “Active Control of Flow Separation Over an Airfoil“, NASA/TM-1999-209838.

[25] Rizzetta, D.P., Visbal, M.R., Stanek, M.J., 1998, "Numerical investigation of synthetic jet flow-fields", 29th AIAA Fluid Dynamics Conference, 98-2910.
[26] Mallinson, S.G., Hong, G., Reizes, J.A., 1999, "Some characteristics of synthetic jets", AIAA 30th Fluid Dynamics Conference, 99-3651.
[27] Meier, G.E.A, 1996, "Active Control of Boundary Layer and Separation", In: Control of Flow Instabilities and Unsteady Flows, Edited by G.E.A. Meier, G.H. Schnerr, Springer, pp.203-234.
[28] Mittal, R., Rampunggoon, P., Udaykumar, H.S., 2002, "Interaction of a Synthetic Jet with a Flat Plate Boundary Layer", AIAA 2001–2773.
[29] Nae, C., 2000, "Unsteady flow control using synthetic jet actuators", AIAA 2000-2403.
[30] Nitsche, M., 1993, "Numerical simulation of axisymmetric vortex sheet roll-up", Vortex flows and related numerical methods, Proc. NATO Advanced Res. Workshop, eds. Beatle, J.T., Collet, G.H., Huberson, S., Kluwer Acad.Publishers.
[31] Safmann, P.G., 1997, "Vortex Dynamics", Cambridge University Press.
[32] Schlichting, H., Gersten, K., 2000, "Boundary Layer Theory", Springer.
[33] Smith, D.R., 2002, "Interaction of a Synthetic Jet with a Crossflow Boundary Layer", AIAA J., vol.40, No.11, November 2002.
[34] Smith, B.L., Glezer, A., 1998, „The formation and evolution of synthetic jets", Physics of Fluids, vol.10, number 9, September 1998, pp.2281-2297.
[35] Smith, B.L., Glezer, A., 2002, "Jet vectoring using synthetic jets", J.Fluid Mech., vol.458, pp.1-34.
[36] Smith, B.L., Swift, G.W., 2003, "A comparison between synthetic jets and continuous jets", Experiments in Fluids, **34**, pp.467–472.
[37] Smith, B.L., Trautman, M.A., Glezer, A., 1999, "Controlled Interactions of Adjacent Synthetic Jets", AIAA 1999-0669.
[38] Takagi, S., Tokugawa, N., Nishizawa, A., "Toward Smart Control of Separation Around a Wing", AIAA.
[39] Trávníček, Z., Tesař, V.,2003, "Annular synthetic jet used for impinging flow mass-transfer", International Journal of Heat and Mass transfer, **46**, 2003, pp.3291–3297.
[40] Uruba, V., 2003, "Synthetic Jets", In: Proceedings of Colloquium FLUID DYNAMICS 2003, IT AS CR, Prague, October 22-24, 2003, pp.163-166.
[41] Uruba, V., 2004, "Synthetic Jet Actuator Design", In: Proceedings of Topical Problems of Fluid Mechanics 2004, February 25, 2004, Prague, pp.169-174.
[42] Wu, K.E., Breuer, K.S., 2003, "Dynamics of Synthetic Jet Actuator Arrays for Flow Control", AIAA.